Mitochondria-Targeted Spin Traps: Synthesis, Superoxide Spin Trapping, and Mitochondrial Uptake

ARTICLE *in* CHEMICAL RESEARCH IN TOXICOLOGY · JUNE 2014

Impact Factor: 3.53 · DOI: 10.1021/tx500032e · Source: PubMed

Chemical Research in Toxicology

Article

pubs.acs.org/crt

Mitochondria-Targeted Spin Traps: Synthesis, Superoxide Spin Trapping, and Mitochondrial Uptake

Micael Hardy,[†] Florent Poulhés,[†] Egon Rizzato,[†] Antal Rockenbauer,[∥] Karol Banaszak,[†] Hakim Karoui,[†] Marcos Lopez,[⊥,#] Jacek Zielonka,[‡,§] Jeannette Vasquez-Vivar,[‡,§] Savitha Sethumadhavan,[‡,§] Balaraman Kalyanaraman,[‡,§] Paul Tordo,*[,†] and Olivier Ouari*[,†]

[†]Aix Marseille Université, CNRS, ICR UMR 7273, 13397 Marseille, France

[‡]Department of Biophysics and [§]Free Radical Research Center, Medical College of Wisconsin, Milwaukee, Wisconsin 53226, United States

[∥]Department of Physics, Budapest University of Technology and Economics and MTA-BME Condensed Matter Research Group, Budafoki ut 8, 1111 Budapest, Hungary

[⊥]Biomedical Translational Research Group, Biotechnology, Fundacion Cardiovascular de Colombia, Floridablanca, Santander, Colombia

[#]Graduate Program of Biomedical Sciences, Faculty of Health, Universidad del Valle, Cali, Colombia

Supporting Information

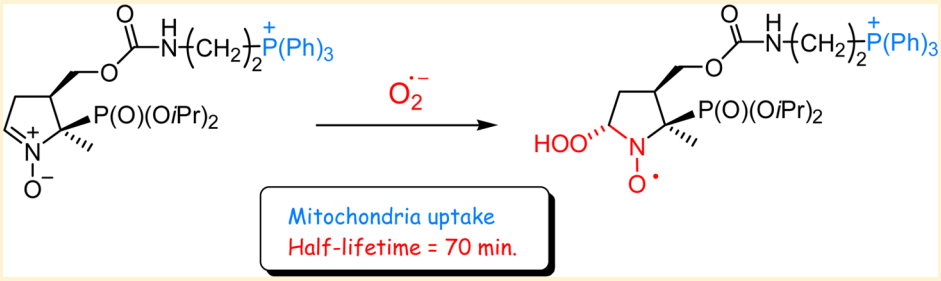

ABSTRACT: Development of reliable methods and site-specific detection of free radicals is an active area of research. Here, we describe the synthesis and radical-trapping properties of new derivatives of DEPMPO and DIPPMPO, bearing a mitochondria-targeting triphenylphosphonium cationic moiety or guanidinium cationic group. All of the spin traps prepared have been observed to efficiently trap superoxide radical anions in a cell-free system. The superoxide spin adducts exhibited similar spectral properties, indicating no significant differences in the geometry of the cyclic nitroxide moieties of the spin adducts. The superoxide adduct stability was measured and observed to be highest ($t_{1/2}$ = 73 min) for DIPPMPO nitrone linked to triphenylphosphonium moiety via a short carbon chain (Mito-DIPPMPO). The experimental results and DFT quantum chemical calculations indicate that the cationic property of the triphenylphosphonium group may be responsible for increased superoxide trapping efficiency and adduct stability of Mito-DIPPMPO, as compared to the DIPPMPO spin trap. The studies of uptake of the synthesized traps into isolated mitochondria indicated the importance of both cationic and lipophilic properties, with the DEPMPO nitrone linked to the triphenylphosphonium moiety via a long carbon chain ($Mito_{10}$-DEPMPO) exhibiting the highest mitochondrial uptake. We conclude that, of the synthesized traps, Mito-DIPPMPO and $Mito_{10}$-DEPMPO are the best candidates for potential mitochondria-specific spin traps for use in biologically relevant systems.

INTRODUCTION

There is increased evidence for the involvement of superoxide radical anions ($O_2^{\bullet-}$) in cell damage and disease via direct effects or through formation of secondary reactive oxygen and nitrogen species (ROS, RNS).[1−3] The role of these species in the pathogenesis and progression of diseases such as atherosclerosis,[4] diabetes,[5] cancer,[6] and neurodegenerative diseases[7,8] is, however, supported by indirect evidence due to the difficulties of direct detection of ROS and RNS in vivo. To gain information on the mechanisms controlling ROS production at the molecular level, the development of new reliable and efficient techniques for their detection[9,10] is needed. Mechanistic studies on the role of $O_2^{\bullet-}$ in oxidative stress processes is made particularly difficult by its low steady-state concentration and the lack of highly specific probes that allow its unequivocal identification and quantification. Electron paramagnetic resonance (EPR) in combination with the spin-trapping technique is the method of choice to detect and characterize radicals such as $O_2^{\bullet-}$.[11−15] In the spin-trapping technique, a spin trap, typically a nitrone or nitroso probe, is introduced into the system under investigation to scavenge

Received: January 30, 2014
Published: June 2, 2014

   dx.doi.org/10.1021/tx500032e | *Chem. Res. Toxicol.* 2014, 27, 1155−1165

Scheme 1. Chemical Structure of Spin Traps 6−12

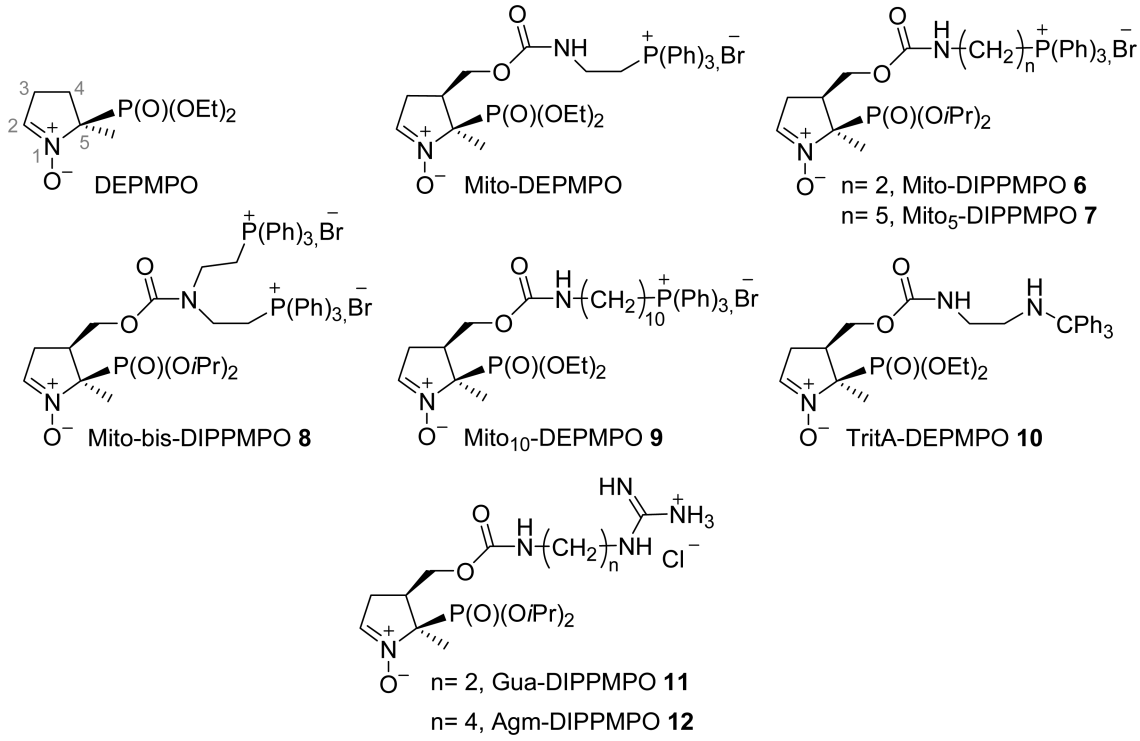

radicals which are too short-lived to be directly detected by EPR. The EPR spectra of the resulting persistent nitroxide spin adducts can usually be recorded, and the spectral analysis can provide valuable information on the chemical identity and dynamics of the radical species produced in the investigated system. However, different drawbacks still limit the use and reliability of the spin trapping for in cell and in vivo studies, and its application to the characterization of $O_2^{\bullet-}$and other oxygen-centered radicals still needs to be improved. Important progress has been made over the last several years, notably with the development of new spin traps that form superoxide spin adducts exhibiting half-lifetimes significantly longer (17−45 min)[16−20] than that observed for the most widely used nitrone spin trap, DMPO (∼1 min).[21−23] Recent research in the oxidative stress field has focused on the development of targeted probes for detecting reactive species in cells.[24,25] Oxygen can be partially reduced by mitochondrial electron transfer protein complexes I and III to $O_2^{\bullet-}$, leading to cell dysfunction.[26,27] Therefore, targeting spin traps to mitochondria might help to characterize the contribution of mitochondrial $O_2^{\bullet-}$. Lipophilic cations such as triphenylphosphonium (TPP^+) and *N*-alkylpyridinium ions have been shown to be effective mitochondria-targeting agents. Their uptake across the mitochondrial inner membrane is enhanced by the mitochondrial membrane potential ($\Delta\Psi$) according to the Nernst equation, with a predicted ∼10-fold accumulation of the cation within mitochondria for every ∼60 mV increase in $\Delta\Psi$.[26,28,29] In recent years, TPP^+-conjugated probes have been used in numerous studies focused on mitochondria-associated responses. For instance, Murphy et al.[30] have determined that MitoQ, a TPP^+-conjugated ubiquinone antioxidant, accumulates up to several-hundred-fold in mitochondria matrix and selectively protected mitochondria, both in vitro and in vivo from the oxidative damage.[31] Mitochondria-targeted cyclic and linear nitrones have been studied, but usually these reagents have limited spin-trapping properties.[29,32,33] Recently, we reported the synthesis and the spin-trapping properties of the TPP^+-conjugated DEPMPO spin trap (Mito-DEPMPO).[16,34] Using this new reagent, we demonstrated that the detection of the superoxide radical anion generated from intact isolated mitochondria is feasible. This result can be explained by the accumulation of Mito-DEPMPO in mitochondria, but we have also shown that, compared with DEPMPO, the rate of trapping of superoxide with Mito-DEPMPO is about two times higher, and that the half-life of the $O_2^{\bullet-}$ adduct is about 2.5 times longer. However, the reasons for these differences between DEPMPO and Mito-DEPMPO are not clear, and we speculated that electrostatic interactions between the TPP^+ cation and the $O_2^{\bullet-}$ or/and the presence of stabilizing H-bonds in the $O_2^{\bullet-}$ adduct might contribute to the observed improvement in superoxide-trapping properties of Mito-DEPMPO.

To better understand the spin-trapping properties of mitochondria-targeted nitrones and to optimize the influence of the TPP^+ cation on the spin trapping of $O_2^{\bullet-}$, we have synthesized a series of Mito-DEPMPO analogues **6**−**12** (Scheme 1). In the series Mito-DIPPMPO **6**, $Mito_5$-DIPPMPO **7**, and $Mito_{10}$-DEPMPO **9**, the length of the linker (C4-$CH_2OC(O)NH(CH_2)_n$-TPP^+) between the C4 and the TPP^+ moiety increases (n = 2, 5, and 10, respectively). Two TPP^+ moieties are present in Mito-bis-DIPPMPO **8** (n = 2), and a neutral $-N(H)CPh_3$ group mimicking the lipophilicity of TPP^+ was introduced in TritA-DEPMPO **10** (n = 2); finally, the TPP^+ cation was replaced by a guanidium group in Gua-DIPPMPO **11** and Agm-DIPPMPO **12** (n = 2 and 4, respectively).

NHS-DIPPMPO and NHS-DEPMPO were used as precursors for the synthesis of the series of derivatives **6**−**12**, illustrating the versatility of the postfunctionalization step

dx.doi.org/10.1021/tx500032e | *Chem. Res. Toxicol.* 2014, 27, 1155−1165

(Scheme 2). For synthetic convenience, NHS-DIPPMPO was mostly used.

Scheme 2[a]

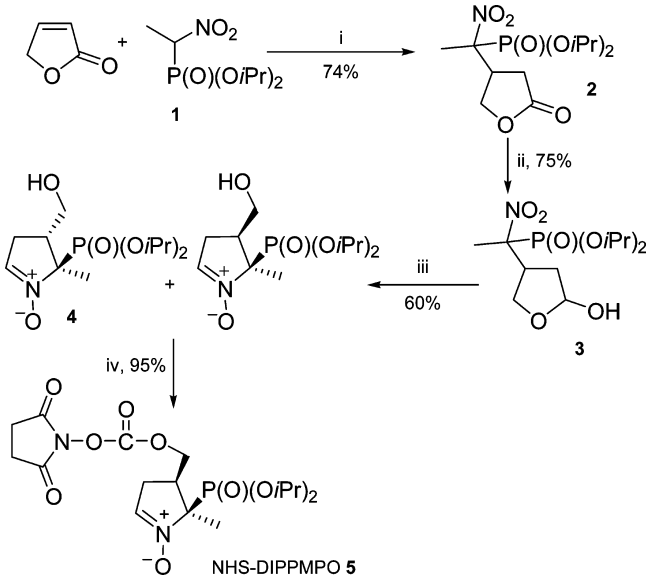

[a]Reagents and conditions: (i) PBu_3, C_6H_{12}/CH_2Cl_2, rt; (ii) DIBAL-H, CH_2Cl_2, −78°C; (iii) Zn/NH_4Cl, H_2O/THF, rt; (iv) DSC, Et_3N, CH_3CN, rt.

Hereafter, we describe the synthesis of compounds **6**−**12**, their spin-trapping properties, and the binding/uptake properties of compounds **6**−**10** to energized mitochondria.

RESULTS AND DISCUSSION

Synthesis. NHS-DIPPMPO **5** was prepared (32% overall yield) in a four-step synthetic sequence (Scheme 2) following the procedure described by Hardy et al.[16] (Supporting Information).

Nitrofuranone **2** was obtained in 74% yield by reacting nitrophosphonate **1** with 2(5*H*)-furanone in the presence of tributylphosphine as catalyst. Reduction of **2** by DIBAL-H at −78 °C led to hemiacetal **3** in good yield (75%). Reductive cyclization of compound **3** in the presence of zinc and ammonium chloride afforded nitrones **4** and **4**′ as a mixture of *cis*/*trans* diastereoisomers, which were separated on silica gel column chromatography (60% yield for **4**). Compound **4** was recrystallized in Et_2O/pentane (8:2), and the geometry obtained by X-ray diffraction confirmed the *cis* position of the diisopropylphosphonyl group relative to the hydroxymethylene moiety (Figure 1).

Reaction of diastereoisomer **4** with *N*,*N*′-disuccinimidyl-carbonate (DSC) in the presence of triethylamine afforded NHS-DIPPMPO **5** in 95% yield.

Compounds **6**−**12** were obtained by reacting NHS-DIPPMPO or NHS-DEPMPO with the amino function of the appropriate side chain, with yields ranging from 50 to 91% (Scheme 3 and Supporting Information).

Except TritA-DIPPMPO **10** and $Mito_{10}$-DEPMPO **9**, all compounds were soluble up to 50 mM concentration in water and in phosphate buffer solutions.

EPR/Spin Trapping. *EPR/Spin Trapping of Superoxide.* The $O_2^{\bullet-}$ trapping properties (Scheme 4) of compounds **6**−**12** were evaluated using two different $O_2^{\bullet-}$-generating systems:

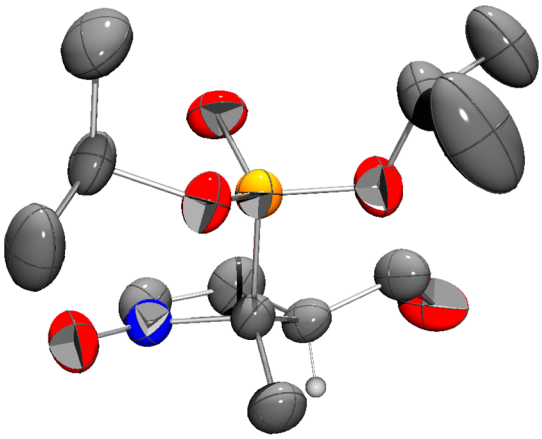

Figure 1. Geometry of compound **4** from X-ray diffraction analysis (Pov-Ray view).

hypoxanthine/xanthine oxidase (HX/XO) and KO_2/18-crown-6-ether/DMSO (KO_2/CE/DMSO) in phosphate buffer. Figure 2 shows the EPR spectra obtained after 10 min incubation of a mixture containing HX (0.4 mM), XO (0.04 U mL^{-1}), DTPA (1 mM), and the spin trap (20 mM of Mito-DIPPMPO; **8** Mito-bis-DIPPMPO; **7** $Mito_5$-DIPPMPO, and **9** $Mito_{10}$-DEPMPO) in oxygen-bubbled phosphate buffer (0.1 M, pH 7.3). The computer-calculated EPR spectra, obtained using the parameters reported in Table 1, are shown as gray lines (Figure 2).

In the presence of superoxide dismutase (SOD), no EPR signal was detected (Figure 2b,d,f,h). Furthermore, for compounds **6**−**9**, identical EPR signals were observed using either the HX/XO or the (KO_2/CE/DMSO) system, the signals being particularly long-lasting with the former. After 30 min, a weak additional signal (<10%) is observable and was assigned to the HO adduct. These results establish that the EPR signals shown in Figure 2 can be unambiguously assigned to the corresponding $O_2^{\bullet-}$ spin adducts.

All spectra appear as doublets (^{31}P coupling) of significantly distorted quartets resulting from close couplings with the ^{14}N and $^1H_\beta$; they were calculated (Table 1) using the EPR/ROKI program.[35] For all of the series, the best fit was obtained assuming that the spin-trapping reaction yields only the *trans*-diastereoisomer (−OOH and $-P(O)(OR)_2$ groups in a *trans* geometry) and the existence of a chemical exchange between two conformational sites T_1 and T_2 composed of rapidly exchanging conformers. In the case of the DEPMPO-OOH and DIPPMPO-OOH spin adducts, the same assumptions were made to account for the dramatic alternate line width observed on the spectra of the *trans*-diastereoisomers.[34−38]

No EPR signals were observed when mixing Agm-DIPPMPO **11** and Gua-DIPPMPO **12** with the HX/XO system. This result is consistent with the inhibitory effect of the guanidine salts on the XO activity.[39] Incubations with KO_2/CE/DMSO led to detection of very similar EPR signals to Mito-DIPPMPO-OOH (Figure 3), confirming the ability of the probes to trap $O_2^{\bullet-}$, consistent with the inhibitory effects of spin traps **11** and **12** on the XO activity.

Within the series of superoxide adduct of compounds **6**−**12**, the values of the determined EPR parameters are similar and close to the values obtained previously for Mito-DEPMPO-OOH (Table 1), suggesting that the modification of the C4 side chain does not significantly change the geometry of the

dx.doi.org/10.1021/tx500032e | *Chem. Res. Toxicol.* 2014, 27, 1155−1165

Scheme 3. Synthesis of Compounds 6−12

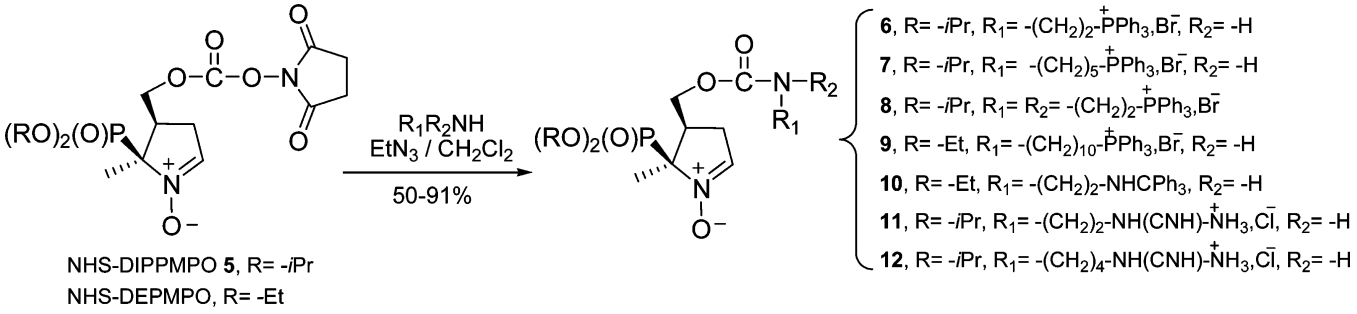

Scheme 4. Spin-Trapping Experiments

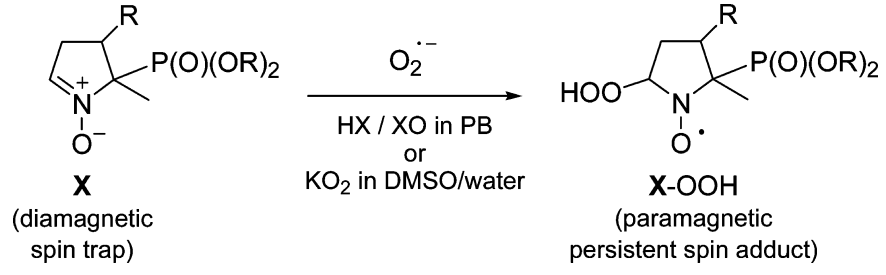

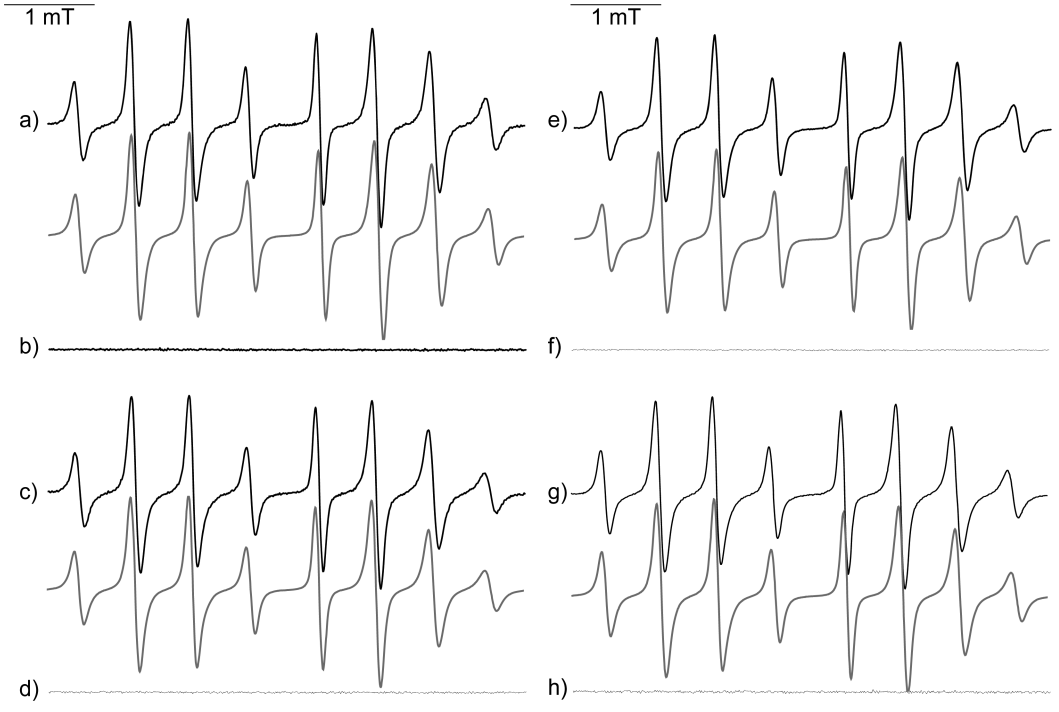

Figure 2. Spin trapping of superoxide radical using Mito-DIPPMPO (**6**), Mito-bis-DIPPMPO (**7**), $Mito_5$-DIPPMPO (**8**), and $Mito_{10}$-DEPMPO (**9**). (a) EPR spectrum obtained after 10 min incubation of a mixture containing hypoxanthine (HX) (0.4 mM), xanthine oxidase (XO) (0.04 U mL^{-1}), DTPA (1 mM), and **6** (20 mM) in oxygen-bubbled phosphate buffer (0.1 M, pH 7.3). (b) Same as in (a) but in the presence of SOD (600 U mL^{-1}). (c) Same as in (a) but containing **7** (20 mM). (d) Same as in (c) but in the presence of SOD (600 U mL^{-1}). (e) Same as in (a) but containing **8** (20 mM). (f) Same as in (e) but in the presence of SOD (600 U mL^{-1}). (g) Same as in (a) but containing **9** (20 mM) and 20% DMSO. (h) Same as in (g) but in the presence of SOD (600 U mL^{-1}). Gray lines: calculated spectra (Table 1). Spectrometer settings: microwave power, 10 mW (a−h); modulation amplitude, 0.7 G (a−h); smooth point, 1 (a−h); gain 75 dB (a−h); sweep time, 41.94 s (a−h); conversion time, 40.96 ms (a−h).

preferred conformers of these spin adducts. However, as it is shown below, the C4 side chain has a strong influence on their stability.

Decay Kinetics of the Superoxide Adduct. Once the concentration of the $O_2^{\bullet-}$ spin adduct has reached a plateau (after ∼9 min), further formation of the $O_2^{\bullet-}$ spin adduct was stopped by the addition of a large amount of SOD and the decay kinetics of the $O_2^{\bullet-}$ adduct was monitored by following the changes in EPR signal intensity. The kinetic studies were performed at 23 °C in 50 μL capillaries, setting the microwave power of the EPR spectrometer at 20 mW. The signal decay was monitored during 70 min, recording successive spectra

dx.doi.org/10.1021/tx500032e | Chem. Res. Toxicol. 2014, 27, 1155−1165

Table 1. Calculated EPR Parameters for the Superoxide Spin Adduct of Mito-DEPMPO and Newly Synthesized Nitrones 6−12

spin adduct	diastereoisomer	site	k (s^{-1})[a]	$\langle a_P \rangle$ (G)	$\langle a_N \rangle$ (G)	$\langle a_{H\beta} \rangle$ (G)
Mito-DEPMPO-OOH	*trans* (100%)	T_1 (70%)	0.1×10^8	53.27	12.79	12.37
		T_2 (30%)		52.01	12.97	10.13
Mito-DIPPMPO-OOH (**6**-OOH)	*trans* (100%)	T_1 (88%)	4.2×10^8	53.41	12.86	12.13
		T_2 (12%)		48.05	12.76	7.38
Mito-bis-DIPPMPO-OOH (**8**-OOH)	*trans* (100%)	T_1 (54%)	2.5×10^8	53.07	12.83	12.17
		T_2 (46%)		45.01	12.69	6.06
$Mito_5$-DIPPMPO-OOH (**7**-OOH)	*trans* (100%)	T_1 (60%)	5.1×10^8	54.03	12.80	12.78
		T_2 (40%)		51.86	12.82	10.57
$Mito_{10}$-DEPMPO-OOH (**9**-OOH)	*trans* (100%)	T_1 (46%)	0.67×10^8	54.54	12.72	14.66
		T_2 (54%)		51.48	12.80	9.00
Agm-DIPPMPO-OOH (**11**-OOH)	*trans* (100%)	T_1 (79%)	0.8×10^7	53.7	12.8	11.9
		T_2 (21%)		51.8	13.3	9.5
Gua-DIPPMPO-OOH (**12**-OOH)	*trans* (100%)	T_1 (74%)	0.35×10^7	53.2	12.8	12.4
		T_2 (26%)		51.5	13.1	9.4

[a]Exchange rate constants in s^{-1}. For DMPO-OOH spin adduct, a theoretical study in an explicit water solution based on a combined QM/MM/MD protocol showed that the EPR spectrum can be explained by two sites in chemical exchange. Moreover, it was demonstrated that each site consists of an equilibrium between the two main five-membered ring conformations of DMPO ($^3T_4$ and $^4T_3$). For all spin adducts, the g values were very close and measured to be 2.006(4).

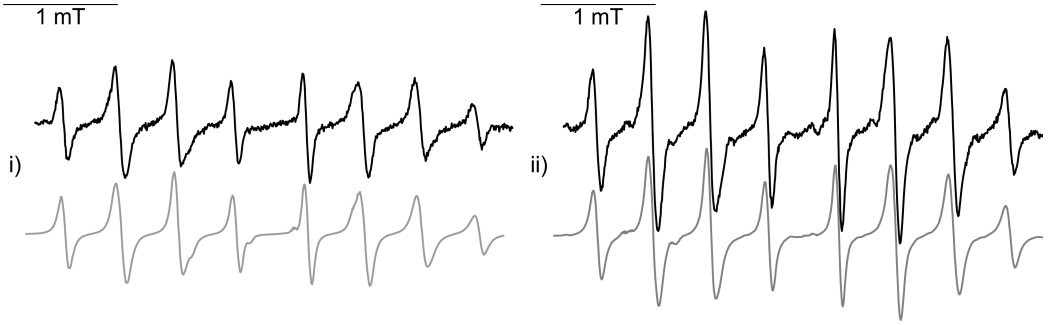

Figure 3. Spin trapping of superoxide radical using Gua-DIPPMPO **11** and Agm-DIPPMPO **12**. (i) EPR spectrum obtained after 2 min incubation of a mixture containing the KO_2/CE/DMSO (5 mM/5 mM/5%) system and **12** (25 mM) in a phosphate buffer (0.1 M, pH 7.3). (ii) Same as in (i) but with **11** (50 mM). Gray lines: calculated spectra (Table 1). Spectrometer settings: microwave power, 10 mW; modulation amplitude, 0.7 G; time constant, 1.28 ms; gain 10^5; sweep time, 21 s; conversion time, 20.48 ms.

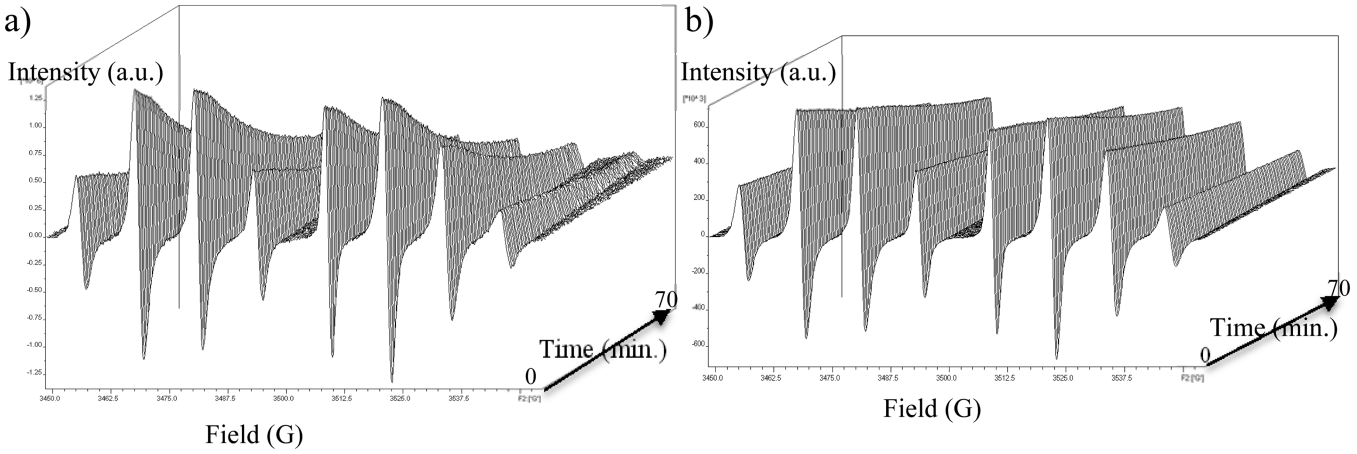

Figure 4. Kinetics of decay of (a) Mito-bis-DIPPMPO-OOH (**8**-OOH) and (b) Mito-DIPPMPO-OOH (**6**-OOH).

every 42 s (Figure 4). All of the recorded spectra were simulated using the Rocky program.[35] The decay curves for the superoxide spin adducts of **6**−**9** are shown in Supporting Information, and the apparent half-lifetimes are listed in Table 2. It is worth noting that the half-lifetime values depend strongly on the experimental conditions and various parameters such as temperature, microwave power, EPR cell (capillaries, AquaX cell) must be carefully controlled in order to get reproducible results.

The values of apparent half-lifetimes ($t_{1/2}$) for the superoxide adducts are reported in Table 2. As one might expect, given the results obtained with Mito-DEPMPO,[16] a ratio of 2.6 was found between the apparent half-lifetime of Mito-DIPPMPO-OOH (n = 2) and that observed with the parent nitrone

dx.doi.org/10.1021/tx500032e | *Chem. Res. Toxicol.* 2014, 27, 1155−1165

Table 2. Apparent Half-Lifetime Values for Superoxide Adducts of DIPPMPO and 6−9 and the Ratio Values of $t_{1/2}$ X-OOH/$t_{1/2}$ DIPPMPO-OOH

spin adducts	$t_{1/2}$ (min)	ratio
DIPPMPO-OOH	28	1
Mito-DIPPMPO-OOH (**6**-OOH)	73	2.61
$Mito_5$-DIPPMPO-OOH (**7**-OOH)	36.6	1.31
Mito-bis-DIPPMPO-OOH (**8**-OOH)	29.3	1.05
DIPPMPO-OOH[a]	25.5	0.91
$Mito_{10}$-DEPMPO-OOH[a] (**9**-OOH)	22	0.78

[a]In 0.1 M phosphate buffer/DMSO mixture (80:20).

DIPPMPO-OOH (this ratio amounts to 2.4−2.5, in the case of Mito-DEPMPO-OOH and DEPMPO-OOH). However, when the spacer arm linking the TPP^+ group and the pyrroline ring was made longer (**7**, $Mito_5$-DIPPMPO, and **9**, $Mito_{10}$-DEPMPO) and when two triphenylphosphonium groups are appended (**8**, Mito-bis-DIPPMPO), the stability of the corresponding superoxide adducts is very close to that observed for the parent nitrone spin adducts. For Agm-DIPPMPO and Gua-DIPPMPO, attempts to perform a kinetic study using the KO_2/CE/DMSO system were frustrated due to the poor reproducibility of the procedure, in addition to decreased persistency of the $O_2^{\bullet-}$ adducts. Measurement of TritA-DEPMPO-OOH (**10**) half-lifetime was not possible because of the low solubility of TritA-DEPMPO.

EPR Characterization of Hydroxyl and 1-Hydroxyethyl Radicals. *Hydroxyl Radical.* When a Fenton system was used in phosphate buffer to generate $HO^\bullet$ in the presence of compounds **6**−**9**, complex signals of low intensity were observed (data not shown). These signals likely correspond to the superimposition of the spectra of hydroxyl spin adducts and the spin adducts of radicals resulting from hydrogen abstraction of $HO^\bullet$ on compounds **6**−**9**. In the presence of an excess of EtOH, hydrogen abstraction generates mainly the 2-hydroxylethyl radical whose spin adducts are clearly identified (Figure 6). These signals are diminished in intensity in the presence of catalase, indicating that these signals depend on hydrogen peroxide breakdown. 12 line EPR spectra corresponding to the $HO^\bullet$ adducts of **6**, **8**, and **9** (Figures 5 and 6) were obtained by reduction of the corresponding superoxide adducts with glutathione peroxidase/glutathione (GPx/GSH), and the hyperfine coupling constants are listed in Table 3.

Quantum-Mechanical Calculations. Under the experimental conditions we used for our spin-trapping experiments, the apparent half-lifetime of Mito-DIPPMPO-OOH is the longest ever observed for the superoxide spin adduct of a spin trap belonging to the pyrroline *N*-oxide series. In an attempt to rationalize this result, we undertook a density functional theory (DFT) approach to the structure of Mito-DIPPMPO (**6**) and Mito-DIPPMPO-OOH (**6**-OOH).

The structures of four conformers ($\mathbf{6}_A$ to $\mathbf{6}_D$; see Supporting Information) have been obtained for **6**, and one of lower energy ($\mathbf{6}_A$) is shown in Figure 7. For all the calculated conformers, the geometry of the pyrroline ring and its two C5 substituents are almost the same and very close to that determined by X-ray diffraction for compound **4** (Figure 1). This geometry is characterized by an envelope at C4 and a pseudoaxial $(i\mathrm{PrO})_2\mathrm{P(O)}$- substituent with its P═O bond directed toward the pyrroline ring. The five calculated conformers differ by the geometry of the C4 substituent. For conformer $\mathbf{6}_A$, the geometry of the $(i\mathrm{PrO})_2\mathrm{P(O)}$- and C4 substituents is in agreement with the *trans* addition of superoxide leading to the observed *trans*-diastereoisomer spin adduct. Furthermore, the kinetics of addition should benefit from the electrostatic interaction of $O_2^{\bullet-}$ with the positive

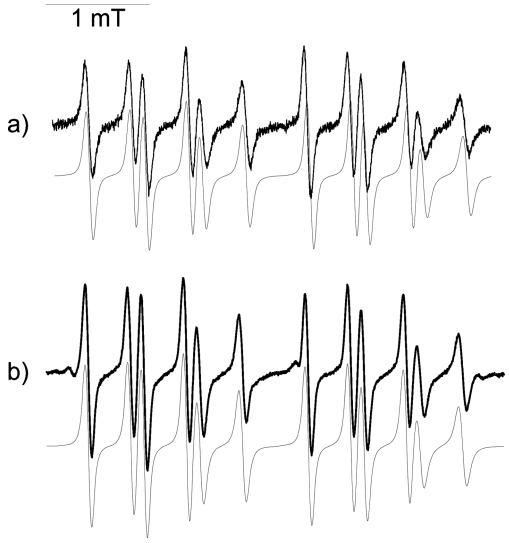

Figure 5. EPR spectra of radical adducts of Mito-bis-DIPPMPO (**8**) and $Mito_{10}$-DEPMPO (**9**). (a) EPR spectrum obtained 10 min after reduction of the **8**-OOH (a) and **9**-OOH (b) adducts (Figure 2) by adding GPx (10 U mL^{-1}) and GSH (1.2 mM) to the incubation mixture and bubbling argon gas for 2 min. Gray lines: calculated spectra (Table 3). Spectrometer settings: microwave power, 30 mW; modulation amplitude, 0.7; time constant, 1.28 ms; gain 10^5; sweep time, 20.4 ms; conversion time, 41.9.

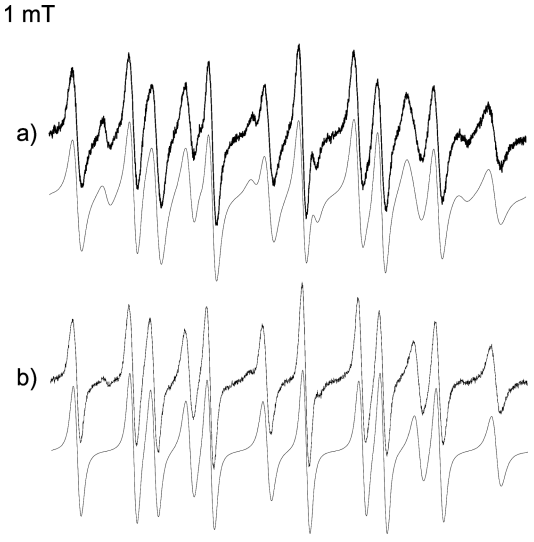

Figure 6. Spin trapping of carbon-centered radical by Mito-bis-DIPPMPO (**8**) and $Mito_{10}$-DEPMPO (**9**). (a) Signal obtained after 15 min incubation of a mixture containing Mito-bis-DIPPMPO (20 mM), H_2O_2 (2 mM), $FeSO_4$ (2 mM), EtOH (15%), and DTPA (1 mM) in phosphate buffer (0.1 M, pH 7.3). (b) Signal obtained after 1 min incubation of a mixture containing $Mito_{10}$-DEPMPO (20 mM), H_2O_2 (2 mM), $FeSO_4$ (2 mM), EtOH (15%), and DTPA (1 mM) in phosphate buffer (0.1 M, pH 7.3). Gray lines: calculated spectra (Table 3). Spectrometer settings: microwave power, 30 mW (a,b); modulation amplitude, 0.7 (a,b); time constant, 1.28 ms (a,b); gain, 10^5 (a,b); sweep time, 20.4 ms (a,b); conversion time, 41.9 (a,b).

dx.doi.org/10.1021/tx500032e | *Chem. Res. Toxicol.* 2014, 27, 1155−1165

Table 3. EPR Parameters of Hydroxyl and Carbon-Centered Spin Adducts

spin adduct	generating system	a_P (G)	a_N (G)	$a_{H\beta}$ (G)
Mito-bis-DIPPMPO-OH	HX/XO and then GPx/GSH	52.4	13.6	10.5
Mito-bis-DIPPMPO-CH(OH)CH_3	Fe^{2+}, H_2O_2, EtOH (15%)	56.8	14.3	19.8
Mito-DIPPMPO-OH	HX/XO and then GPx/GSH	53.1	13.6	10.5
Mito-DIPPMPO-CH(OH)CH_3	Fe^{2+}, H_2O_2, EtOH (15%)	57.5	14.3	19.7
$Mito_{10}$-DEPMPO-OH	HX/XO and then GPx/GSH	52.9	13.4	10.2
$Mito_{10}$-DEPMPO-CH(OH)CH_3	Fe^{2+}, H_2O_2, EtOH (5%)	57.6	14.2	19.4

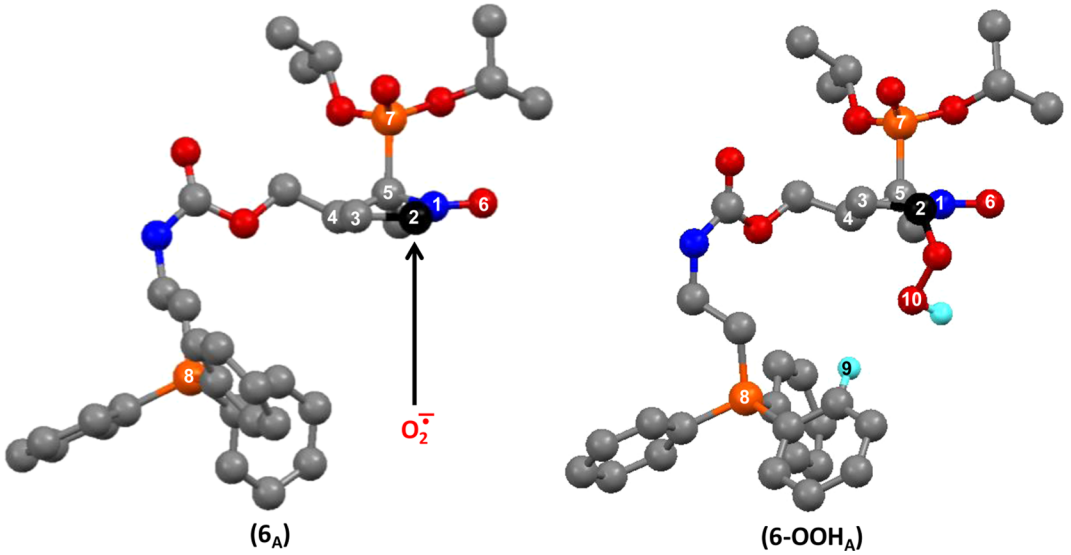

Figure 7. Calculated DFT [B3LYP-6-31G(d,p), PCM (water)] structures of the lowest energy conformers of Mito-DIPPMPO ($\mathbf{6}_A$) and Mito-DIPPMPO-OOH (**6**-OOH_A).

charges brought by the TPP^+ moiety, and we indeed observed that it increases by a factor 2 compared with DIPPMPO.

The structures of four conformers **6**-OOH_A to **6**-OOH_D (Figure 7 and Supporting Information) have been obtained for the superoxide adduct of DIPPMPO. The conformers **6**-$OOH_{A,B,C}$ correspond to the *trans* addition of superoxide to **6**, and their energies are very close (ΔE_{max} = 2.93 kJ·mol^{-1}). For these three conformers, the positively charged phosphorus atom P8 is close to the hydroperoxyl group (P_8-O_{10} = 4.94 Å for **6**-OOH_A, Figure 7), and stabilizing interactions can be established between the positive hydrogen atoms (d = +0.31, Mulliken charge) of one phenyl group and the oxygen lone pairs (H_9-O_{10} = 2.51 Å for **6**-OOH_A, Figure 7). These interactions of the TPP^+ moiety with the hydroperoxyl group likely contribute to the stabilization of the species, resulting in the especially long half-lifetime observed. For conformer **6**-OOH_D, the distance P_8-O_{10} is much higher (10.53 Å) and its energy is 6.10 to 9.02 kJ·mol^{-1} higher compared to that of conformers **6**-$OOH_{A,B,C}$. For these latter conformers, the agreement between the calculated and the experimental hyperfine coupling constants is satisfying [for **6**-OOH_A, the lowest energy conformer, A_N = 1.00 mT $(1.28)_{exp}$; A_P = 5.00 mT $(5.27)_{exp}$; $A_{H\beta}$ = 1.13 mT $(1.17)_{exp}$].

Mitochondrial Uptake Studies. The mitochondrial binding/uptake of compounds **6**–**10** was evaluated from the decrease of the compounds' concentration after incubation during 30 min with respiring mitochondria. No kinetic study was performed, and the method was based on the quantification of the compounds remaining in the supernatant (see Experimental Section). The results of mitochondrial uptake experiments reported in Table 4 represent the percentage of decrease in compounds' concentration during incubation with energized (with succinate) mitochondria, as compared to mitochondria without succinate. The effects of triphenylphosphonium (TPP^+) in improving their affinity for mitochondria is clear from the investigated series, where little effects are seen for DIPPMPO and no membrane potential-dependent uptake is observed for TritA-DEPMPO **10**. We conclude that highly delocalized cationic charge on the lipophilic phenyl rings is necessary for the accumulation in mitochondria in membrane potential-dependent manner. Surprisingly, the presence of two TPP^+ in Mito-bis-DIPPMPO **8** did not increase the uptake, which may be due to the close vicinity of the two moieties.[40] The best uptake was obtained with $Mito_{10}$-DEPMPO **9**, probably due its higher hydrophobicity and amphiphilic properties. The mitochondrial uptake of $Mito_{10}$-DEPMPO **9** and Mito-bis-DIPPMPO **8** has been independently confirmed by LC-MS/MS analysis of the extracts of mitochondrial pellets, indicating significantly higher accumulation of compounds **8** and **9**, as compared to the nontargeted spin trap, DIPPMPO (data not shown).

Table 4. Percentage of Mitochondria Uptake Determined by HPLC/UV–Vis Detection

spin traps	mitochondrial uptake (%)
DIPPMPO	2.4
Mito-DIPPMPO (**6**)	29
$Mito_5$-DIPPMPO (**7**)	21.1
$Mito_{10}$-DEPMPO (**9**)	58
Mito-bis-DIPPMPO (**8**)	25.6
TritA-DEPMPO (**10**)	0

dx.doi.org/10.1021/tx500032e | *Chem. Res. Toxicol.* 2014, 27, 1155–1165

CONCLUSIONS

With the aim to develop tools for the study of $O_2^{\bullet-}$ formation in mitochondria, we have prepared a series of DIPPMPO and DEPMPO derivatives, with a substituent in the 4-position of the pyrroline ring, having different lengths and bearing a TPP^+ cation or a guanidinium group as the chain end. We have studied the spin-trapping properties of these new spin traps and determined their mitochondria uptake. All of the compounds bearing a TPP^+ cation efficiently react with $O_2^{\bullet-}$, forming stable adducts. The results of quantum-mechanical calculations suggest that the addition of the negatively charged $O_2^{\bullet-}$ to Mito-DIPPMPO could be facilitated by the attraction exerted by the TPP^+ group. Moreover, in the most stable conformers of Mito-DIPPMPO-OOH, the interactions of the TPP^+ moiety with the hydroperoxyl group likely contribute to the stabilization of the species, resulting in the especially long half-lifetime observed.

Results from the mitochondria uptake studies showed the key role of the TPP^+ moiety in the targeting properties. It should be noted, however, that other factors such as the accessibility of the TPP^+ group or the amphiphilic properties of the molecule can modulate the mitochondria uptake, which cannot readily be predicted, and experimental determination is required. Spin traps that can be compartmentalized or localized at particular biological sites are part of the toolbox required for maximizing the amount of useful information, as it is now clear that data obtained from multiple techniques are often required to obtain a definitive picture on the formation and role of free radicals in biological systems. The apparent half-lifetime of the $O_2^{\bullet-}$ adduct and the mitochondrial uptake are 73 min and 30% for Mito-DIPPMPO (**6**) and 22 min and 60% for $Mito_{10}$-DEPMPO (**9**), making these new spin traps suitable candidates for mitochondrial superoxide trapping.

EXPERIMENTAL SECTION

Materials. CH_2Cl_2 was distilled under dry argon atmosphere in the presence of P_2O_5. All reagents were used as received without further purification. The reactions were monitored by TLC on silica gel and by ^{31}P NMR. Crude materials were purified by flash chromatography on silica gel 60 (0.040−0.063 mm). ^{31}P NMR, ^1H NMR, and ^{13}C NMR spectra were recorded with 300 or 400 spectrometers at 121.49, 300.13, and 75.54 MHz, respectively. ^{31}P NMR data were taken in $CDCl_3$ using 85% H_3PO_4 as an external standard with broad-band ^1H decoupling. ^1H NMR and ^{13}C NMR data were taken in $CDCl_3$ using TMS or $CDCl_3$ as internal reference, respectively. Chemical shifts (δ) are reported in parts per million and coupling constant J values in Hertz. The assignments of NMR signals were facilitated by use of the DEPT 135 sequence for all of the nitrones. High-resolution MS (HRMS) experiments were performed with a mass spectrometer equipped with an electrospray ionization source operated in the positive ion mode. In this hybrid instrument, ions were measured using an orthogonal acceleration time-of-flight (oa-TOF) mass analyzer.

Synthesis of Nitrone NHS-DIPPMPO 5. The synthesis was performed by adapting the procedure described by Hardy et al.[41] The nitrophosphonate **1** has already been described.[42]

4-(1-Diisopropyloxyphosphoryl-1-nitroethyl)tetrahydrofuran-2-one ***2***. Product **2** was obtained as a yellow oil (25 g, 74%) corresponding to a mixture of two diastereoisomers: ^{31}P NMR (121.49 MHz) δ 12.84 (60%), 12.95 (40%); ^1H NMR (300.13 MHz) δ 1.40−1.30 (12H, m), 1.75 (3H, d, J = 14.4), 2.74−2.36 (2H, m), 3.82−3.63 (1H, m), 4.54−4.07 (2H, m), 4.86−4.66 (2H, m); ^{13}C NMR (75.47 MHz) δ 174.7 (C^{IV}, s), 174.6 (C^{IV}, s), 90.5 (C^{IV}, d, J = 148.0), 90.2 (d, J = 147.1), 74.4 (s), 74.3 (s), 74.2 (d, J = 1.8), 74.0 (d, J = 1.4), 68.4 (d, J = 2.8), 68.2 (s), 40.2 (s), 39.7 (s), 30.3 (d, J = 2.8), 29.9 (d, J = 8.3), 24.1 (d, J = 3.2), 23.9 (d, J = 1.8), 23.8 (d, J = 1.8), 23.5 (d, J = 1.4), 23.4 (s), 23.3 (d, J = 1.4), 16.2 (d, J = 1.4), 16.1 (d, J = 1.4); HMRS calcd for $C_{12}H_{22}NO_7P$, $[C_{12}H_{22}NO_7P + NH_4]^+$, 341.1472; found 341.1474.

4-(1-Diisopropyloxyphosphoryl-1-nitroethyl)-2-hydroxytetrahydrofuran ***3***. Product **3** was obtained as a yellow oil (3 g, 75%) corresponding to a mixture of four diastereoisomers: ^{31}P NMR (121.49 MHz) δ 14.58 (44%), 14.75 (22%), 14.95 (34%); ^1H NMR (300.13 MHz) δ 1.40−1.25 (12H, m), 1.66 and 1.78 and 1.83 (3H, 3d, J = 14.4, 14.5, 14,0), 1.98−1.87 (1H, m), 3.57−3.32 (1H, m), 3.94−3.60 (2H, m), 4.21−4.01 (1H, m), 4.85−4.62 (2H, m), 5.51 (1H, t, J = 3.2); ^{13}C NMR (75.47 MHz) δ 97.8 (s), 97.7 (s), 91.4 (C^{IV}, d, J = 148.4), 73.8 (d, J = 6.7), 73.7 (d, J = 6.7), 73.5 (d, J = 7.3), 67.1 (d, J = 0.9), 66.9 (d, J = 0.9), 43.0 (s), 42.3 (s), 35.2, (s), 34.9 (s), 34.8 (s), 24.2 (d, J = 7.8), 24.5 (d, J = 5.0), 24.4 (d, J = 5.9), 15.2 (s), 14.9 (s); HMRS calcd for $C_{12}H_{24}NO_7P$, $[C_{12}H_{22}NO_7P + H]^+$, 326.1363; found 326.1363.

5-Diisopropyloxyphosphoryl-5-methyl-4-hydroxymethyl-1-pyrroline N-Oxide ***4*** *and* ***4′***. Nitrones **4** and **4′** were obtained in 60% yield (7 g) corresponding to a mixture of two diastereoisomers. (4*R**,5*R**)-4-HMDIPPMPO **4**: ^{31}P NMR (121.49 MHz) δ 21.19; ^1H NMR (300.13 MHz) δ 1.31 (3H, d, J = 6.2), 1.32 (3H, d, J = 6.0), 1.37 (3H, d, J = 6.2), 1.41 (3H, d, J = 6.2), 1.70 (3H, d, J = 14.5), 2.75−2.37 (3H, m), 3.92−3.82 (2H, m), 4.18 (1H, m), 4.95−4.71 (2H, m), 6.88 (1H, dt, J = 2.4, 2.4); ^{13}C NMR (75.47 MHz) δ 134.1 (1C, d, J = 7.7), 77.0 (1C, d, J = 152.0), 73.3 (1C, d, J = 7.1), 72.8 (1C, d, J = 7.7), 62.4 (1C, d, J = 5.5), 49.3 (1C, d, J = 5.7), 29.2 (1C, s), 24.2 (1C, d, J = 2.7), 24.0 (1C, d, J = 2.7), 24.8 (1C, d, J = 6.0), 23.6 (1C, d, J = 5.5), 21.4 (1C, d, J = 1.6); ESI-MS m/z 293 $[M + H]^+$; HMRS calcd for $C_{12}H_{24}NO_5P$, $[C_{12}H_{25}NO_5P + H]^+$, 294.1465; found 294.1465. (4*S**,5*R**)-4-HMDIPPMPO **4′**: ^{31}P NMR (121.49 MHz) δ 21.97; ^1H NMR (300.13 MHz) δ 1.31 and 1.32 (12H, 2d, J = 6.2, 6.2), 1.57 (3H, d, J = 16.0), 2.60−2.34 (2H, m), 3.14−2.72 (2H, m), 3.79−3.69 (1H, m), 4.2−3.90 (1H, m), 4.90−4.67 (2H, m), 6.82 (1H, dt, J = 2.7, 2.6); ^{13}C NMR (75.47 MHz) δ 134.2 (1C, d, J = 8.8), 76.7 (1C, d, J = 159.7), 73.0 (1C, d, J = 7.1), 72.1 (1C, d, J = 7.7), 61.4 (1C, d, J = 6.0), 40.9 (1C, s), 30.0 (1C, d, J = 4.9), 24.2 (1C, d, J = 2.7), 23.9 (1C, d, J = 4.4), 23.8 (1C, d, J = 4.9), 23.5 (1C, d, J = 6.6), 14.2 (1C, s).

(4R,5R*)-5-Diisopropyloxyphosphoryl-5-methyl-4-(succinimidyloxycarbonyloxymethyl)-1-pyrroline N-Oxide* ***5***. Nitrone NHS-DIPPMPO **5** was obtained as a white crystal (1.4 g, 100%): ^{31}P NMR (81.01 MHz) δ 18.0; ^1H NMR (300.13 MHz) δ 1.41−1.26 (12H, m), 1.66 (3H, d, J = 14.0), 2.90−2.63 (3H, m), 2.8 (4H, s), 4.63−4.48 (1H, m), 4.86−4.67 (3H, m), 6.92 (1H, m); ^{13}C NMR (50.32 MHz) δ 168.5 (2C, s), 151.3 (1C, s), 133.5 (1C, d, J = 7.3), 75.9 (1C, d, J = 149.8), 73.9 (1C, d, J = 6.4), 72.1 (1C, d, J = 7.8), 70.5 (1C, d, J = 3.2), 45.6 (1C, d, J = 2.3), 30.0 (1C, d, J = 0.9), 25.4 (2C, s), 24.5 (1C, d, J = 1.4), 23.8 (1C, d, J = 1.4), 23.7 (1C, d, J = 1.8), 23.4 (1C, d, J = 7.3), 20.3 (1C, s); HMRS calcd for $C_{17}H_{27}N_2O_9P$, $[C_{17}H_{27}N_2O_9P + H]^+$, 435.1527; found 435.1527.

Synthesis of the Nitrone Mito-DIPPMPO 6. *Mito-DIPPMPO* ***6***. To a mixture of NHS-DIPPMPO (0.2 g, 0.46 mmol) and (2-aminoethyl)triphenylphosphonium bromide (0.18 g, 0.46 mmol) in CH_2Cl_2 (15 mL) was added at room temperature under inert atmosphere triethylamine (141 μL, 1.06 mmol). The reaction mixture was stirred for 3 h. The solution was washed with 8 mL of distilled water and extracted three times with $CHCl_3$. The organic layers were dried over Na_2SO_4, and the solvent distilled under reduced pressure. Purification of the crude product by flash chromatography on silica gel (CH_2Cl_2/EtOH 80:20) afforded a white powder (0.28 g, 86%), corresponding to Mito-DIPPMPO **6**: ^{31}P NMR (121.49 MHz) δ 17.8, 20.9; ^1H NMR (300.13 MHz) δ 1.38−1.27 (12H, m), 1.62 (3H, d, J = 14.1), 2.68−2.52 (3H, broad band), 3.57−3.68 (2H, m), 3.95−3.33 (2H, m), 4.17−4.07 (1H, m), 4.36−4.29 (1H, m), 4.79−4.67 (2H, m), 6.91 (1H, m), 7.52 (1H, t, J = 6.0), 7.82−7.63 (15H, broad band); ^{13}C NMR (75.47 MHz) δ 156.5 (1C, s), 135.2 (3C, d, J = 2.9), 134.6 (1C, d, J = 7.3), 133.6 (6C, d, J = 10.3), 130.5 (6C, d, J = 12.4), 117.5 (3C, d, J = 86.5), 75.1 (1C, d, J = 149.6), 73.4 (1C, d, J = 6.6), 71.8 (1C, d, J = 8.0), 64.5 (1C, s), 46.4 (1C, d, J = 2.2), 35.2 (1C, s), 30.7 (1C, s), 24.5 (1C, d, J = 1.5), 24.0 (1C, d, J = 3.7), 25.8 (1C, d, J = 5.1), 23.6

(1C, d, J = 7.3), 23.3 (1C d, J = 48.4), 20.3 (1C, s); HMRS calcd for $[C_{33}H_{43}N_2O_6P_2]^+$, Br^-, $[C_{33}H_{43}N_2O_6P_2]^+$, 625.2591; found 625.2587.

Synthesis of Nitrone Mito-bis-DIPPMPO 8. *Bis-[2-(triphenylphosphonium bromide)ethyl]amine* ***A***. A mixture containing bis(2-bromoethyl)amine[43] (7 g, 0.03 mol) and triphenylphosphane (16 g, 0.061 mol) in acetonitrile (50 mL) was refluxed for 48 h. The solvent was distilled under reduced pressure. Purification of the crude product by flash chromatography on a silica gel (CH_2Cl_2/EtOH 80:20) afforded a brown solid **A** (12 g, 52%): ^{31}P NMR (121.49 MHz) δ 23.56; ^{1}H NMR (300.13 MHz) δ 3.06−3.12 (4H, m), 3.72−3.80 (4H, m), 7.60−7.82 (30H, m); ^{13}C NMR (75.47 MHz) δ 134.6 (6C, d, J = 2.9), 133.8 (12C, d, J = 10.3), 130.4 (12C, d, J = 12.5), 118.5 (6C, d, J = 86.6), 41.7 (2C, s), 23.7 (2C, d, J = 50.6); ESI-MS m/z 297.6 $[M + H]^{++}$.

Mito-bis-DIPPMPO ***8***. To a mixture of NHS-DIPPMPO (0.2 g, 0.46 mmol) and bis[2-(triphenylphosphonium bromide)ethyl]amine **A** (0.37 g, 0.46 mmol) in CH_2Cl_2 (5 mL) was added at room temperature under inert atmosphere triethylamine (141 μL, 1.06 mmol). The reaction mixture was stirred for 3 h. The solution was washed with 8 mL of distilled water and extracted three times with $CHCl_3$. The organic layers were combined and dried over Na_2SO_4, and the solvent was removed under reduce pressure. Purification of the crude product by flash chromatography on silica gel (CH_2Cl_2/EtOH 80:20) afforded a white powder (0.25 g, 50%), corresponding to Mito-bis-DIPPMPO **8**: ^{31}P NMR (121.49 MHz) δ 17.61, 21.89; ^{1}H NMR (300.13 MHz) δ 1.38−1.26 (12H, m), 1.53 (3H, d, J = 13.8), 2.82−2.62 (3H, m), 4.10−3.90 (4H, m), 4.35−4.12 (4H, m), 4.60−4.39 (2H, m), 4.79−4.62 (2H, m), 6.83 (1H, m), 7.60−7.98 (30H, m); ^{13}C NMR (75.47 MHz) δ 154.9 (1C, s), 134.8 (3C, d, J = 2.9), 134.7 (3C, d, J = 2.9), 134.6 (1C, d, J = 8.8), 134.2 (6C, d, J = 7.3), 134.1 (6C, d, J = 7.3), 130.4 (6C, d, J = 12.5), 130.3 (6C, d, J = 12.5), 117.9 (3C, d, J = 86.6), 117.8 (3C, d, J = 86.8), 75.8 (1C, d, J = 149.6), 73.5 (1C, d, J = 6.6), 71.7 (1C, d, J = 7.3), 64.3 (1C, d, J = 2.2), 45.8 (1C, d, J = 2.2), 42.9 (1C, s), 42.6 (1C, s), 29.2 (1C, s), 24.5 (1C, s), 24.0 (1C, d, J = 4.4), 23.9 (1C, d, J = 4.4), 23.4 (1C, d, J = 7.3), 23.1 (1C, d, J = 46.2), 22.1 (1C, d, J = 47.7), 20.3 (1C, s); HMRS calcd for $[C_{53}H_{61}N_2O_6P_3]^{2+}$, $2Br^-$, $[C_{53}H_{61}N_2O_6P_3]^{2+}$, 457.1866; found 457.1868.

Synthesis of Nitrone Mito$_5$-DIPPMPO 7. *Mito$_5$-DIPPMPO* ***7***. To a mixture of NHS-DIPPMPO (0.200 g, 0.46 mmol) and (2-aminopentyl)triphenylphosphonium bromide[44] (0.190 g, 0.46 mmol) in CH_2Cl_2 (20 mL) was added at room temperature under inert atmosphere triethylamine (147 μL, 6 mmol). The reaction mixture was stirred for 3 h. The solution was washed with 8 mL of distilled water and extracted three times with $CHCl_3$. The organic layers were combined and dried over Na_2SO_4, and the solvent was removed under reduce pressure. Purification of the crude product by flash chromatography on silica gel (CH_2Cl_2/EtOH 80:20) afforded a white powder (0.171 g, 50%), corresponding to Mito$_5$-DIPPMPO **7**: ^{31}P NMR (121.49 MHz) δ 18.0, 24.3; ^{1}H NMR (300.13 MHz) δ 1.38−1.26 (12H, m), 1.62 (3H, d, J = 14.0), 1.71−1.57 (6H, m), 2.72−2.61 (3H, broad band), 3.13−3.09 (2H, m), 3.73−3.66 (2H, m), 4.21−4.16 (1H, m), 4.45−4.40 (1H, m), 4.77−4.69 (2H, m), 6.29 (1H, t, J = 5.5), 6.91 (1H, m), 7.82−7.63 (15 H, broad band); ^{13}C NMR (75.47 MHz) δ 156.6 (1C, s), 135.0 (3C, d, J = 2.9), 135.5 (6C, d, J = 10.3), 130.4 (6C, d, J = 12.5), 118.2 (3C, d, J = 85.8), 75.9 (1C, d, J = 150.4), 73.2 (1C, d, J = 6.6), 71.6 (1C, d, J = 7.3), 64.0 (1C, s), 46.5 (1C, d, J = 2.2), 39.9 (1C, s), 30.7 (1C, s), 29.5 (1C, s), 28.3 (1C, s), 26.9 (1C, d, J = 16.7), 24.5 (1C, d, J = 1.5), 23.9 (1C, d, J = 3.7), 23.7 (1C, d, J = 5.4), 23.4 (1C, d, J = 6.6), 22.5 (1C, d, J = 49.9), 21.8 (1C, d, J = 4.4), 20.3 (1C, s); HMRS calcd for $[C_{36}H_{49}N_2O_6P_2]^+$, Br^-, $[C_{36}H_{49}N_2O_6P_2]^+$, 667.3060; found 667.3060.

Synthesis of Nitrone Mito$_{10}$-DEPMPO 9. *(10-Phthalimidodecyl)triphenylphosphonium Bromide* ***B***. A mixture containing bromophthalimide (7 g, 0.019 mol) and triphenylphosphane (5 g, 0.019 mol) in acetonitrile (60 mL) was refluxed for 15 h. The solvent was distilled under reduced pressure. Purification of the crude product by flash chromatography on a silica gel (CH_2Cl_2/EtOH 80:20) afforded a white solid **B** (9 g, 73%): MS calcd for $[C_{36}H_{39}NO_2P]^+$, Br^-, $[C_{36}H_{39}NO_2P]^+$, 548.3; found 548.3.

(10-Aminodecyl)triphenylphosphonium Bromide ***C***. To a solution of **B** (7 g, 0.011 mol) in EtOH (70 mL) was added hydrazine (0.54 mL, 0.011 mol). The mixture was refluxed for 15 h. The solvent is distilled, and the impurity was recrystallized using a mixture Et_2O/EtOH (2/1). The product purified by flash chromatography on silica gel (CH_2Cl_2/EtOH 80:20) afforded a yellow solid **C** (4 g, 73%): ^{31}P NMR (121.49 MHz) δ 24.61; ^{1}H NMR (300.13 MHz) δ 7.95−7.73 (15H, m), 3.70−3.55 (2H, m), 2.80−2.70 (2H, m), 1.60−1.40 (6H, m), 1.35−1.10 (10H, m). MS calcd for $[C_{28}H_{37}NP]^+$, Br^-, $[C_{28}H_{37}NP]^+$, 418.2; found 418.2.

Mito$_{10}$-DEPMPO ***9***. To a mixture of NHS-DEPMPO (0.25 g, 0.61 mmol) and (10-aminodecyl)triphenylphosphonium bromide **C** (0.32 g, 0.62 mmol) in CH_2Cl_2 (20 mL) was added at room temperature under inert atmosphere triethylamine (0.23 mL, 1.61 mmol). The reaction mixture was stirred for 3 h and then washed with water (15 mL). The organic layer was dried over Na_2SO_4, and the solvent was distilled under reduce pressure. Purification of the crude product by flash chromatography on silica gel (CH_2Cl_2/EtOH 70:30) afforded a white powder (0.31 g, 64%), corresponding to Mito$_{10}$-DEPMPO **9**: ^{31}P NMR (121.49 MHz) δ 20.58, 25.48; ^{1}H NMR (300.13 MHz) δ 1.39−1.16 (17H, m), 1.50−1.40 (2H, m), 1.65−1.57 (3H, m), 1.68 (3H, d, J = 14.0), 2.80−2.55 (3H, m), 3.19−3.06 (2H, m), 3.90−3.60 (3H, m), 4.30−4.10 (5H, m), 4.56−4.45 (1H, m), 6.97 (1H, dt, J = 2.4, 2.4), 7.92−7.62 (15H, m); ^{13}C NMR (75.47 MHz) δ 156.1 ($1C^{IV}$, s), 134.8 (1C, d, J = 8.2), 134.9 (3C, d, J = 3), 133.7 (6C, d, J = 9.7), 130.4 (6C, d, J = 12.6), 118.5 ($3C^{IV}$, d, J = 85.5), 76.2 (1C, d, J = 155.7), 64.3 (1C, d, J = 6.3), 63.9 (1C, s), 62.5 (1C, d, J = 8.0), 46.7 (1C, d, J = 2.3), 41.0 (1C, s), 30.4 (1C, s), 30.2 (1C, s), 29.7 (1C, s), 29.0 (1C, s), 28.9 (2C, s), 26.52 (1C, s), 23.0 (1C, d, J = 49.3), 22.6 (1C, d, J = 4.0), 22.7 (1C, d, J = 49.3), 20.3 (1C, s), 16.4 (1C, d, J = 5.7), 16.3 (1C, d, J = 5.7); HRMS calcd for $[C_{39}H_{55}N_2O_6P_2]^+$, Br^-, $[C_{39}H_{55}N_2O_6P_2]^+$, 709.3530; found 709.3529.

Synthesis of Nitrone TritA-DEPMPO 10. *TritA-DEPMPO* ***10***. To a mixture of NHS-DEPMPO (0.15 g, 3.6 mmol) and *N*-tritylethylenediamine hydrobromide (0.14 g, 3.6 mmol) in CH_2Cl_2 (10 mL) was added triethylamine (103 μL, 1.61 mmol) at room temperature under argon. The reaction mixture was stirred for 5 h and then washed with water (15 mL). The organic layer was dried over Na_2SO_4, and the solvent was distilled under reduced pressure. Purification of the crude product by flash chromatography on a silica gel (CH_2Cl_2/EtOH 97:03) afforded a white powder (0.2 g, 91%), corresponding to TritA-DEPMPO **10**: ^{31}P NMR (121.49 MHz) δ 19.75; ^{1}H NMR (300.13 MHz) δ 7.49−7.43 (5H, m), 7.33−7.28 (4H, m), 7.27−7.20 (6H, m), 7.18 (1H, t, J = 1.2), 7.01 (1H, m), 5.08 (1H, t, J = 4.2), 4.62−4.53 (1H, m), 4.38−4.12 (5H, m), 3.37−3.21 (2H, m), 2.84−2.57 (3H, m), 2.30 (2H, t, J = 6.0), 1.73 (3H, d, J = 14.0), 1.36 (6H, dt, J = 7.0); ^{13}C NMR (75.47 MHz) δ 156.1 ($1C^{IV}$, s), 145.7 ($3C^{IV}$, s), 134.5 (1C, d, J = 8.0), 128.5 (6C, s), 127.9 (6C, s), 126.4 (3C, s), 76.1 (1C, d, J = 160.6), 70.6 ($1C^{IV}$, s), 64.3 (1C, d, J = 6.3), 64.1 (1C, s), 62.4 (1C, d, J = 7.4) 46.7 (1C, s), 43.6 (1C, s), 41.7 (1C, s), 30.3 (1C, s), 20.3 (1C, s), 16.3 (1C, d, J = 5.7), 16.2 (1C, d, J = 5.7); HRMS calcd for $[C_{32}H_{40}N_3O_6P]$, $[C_{32}H_{40}N_2O_6P]^+$, 594.2728; found 594.2735.

Synthesis of Nitrone Gua-DIPPMPO 11. *Gua-DIPPMPO* ***11***. To a mixture of (2-aminoethyl)guanidine (0.13 g, 1,1 mmol) in acetonitrile (5 mL) was added NHS-DIPPMPO **5** (0.4 g, 0.92 mmol) in 10 mL of anhydrous acetonitrile following by the addition of *N*-ethyldiisopropylamine (0,24 mL, 1,38 mmol). The reaction mixture was stirred overnight. The solvent was removed under reduce pressure. Purification of the crude product by flash chromatography on basic alumina (CH_2Cl_2/EtOH 85:15) afforded a pale yellow powder (0.23 g, 60%): ^{31}P NMR (121.49 MHz, D_2O) δ 17.81; ^{1}H NMR (300.13 MHz) δ 6.91 (1H, d, J = 3.02), 4.78−4.67 (2H, m), 4.59−4.53 (1H, m), 4.41−4.35 (1H, m), 3.87−3.69 (2H, m), 3.65−3.57 (2H, m), 2.78−2.52 (3H, m), 1.64 (3H, d, J = 14), 1.35−1.27 (12H, m); ^{13}C NMR (75.47 MHz) δ 161.5 ($1C^{IV}$, s), 158.5 (1C, s), 144.7 (1C, d, J = 8.0), 76.6 ($1C^{IV}$, d, J = 153.74 Hz), 75.7 (1C, d, J = 8.0), 75.58 (1C, d, J = 8.0), 61.8 (1C, d, J = 3.5), 49.1 (1C, d, J = 2.3), 43.4 (2C, s), 31.7 (1C, s), 24.1 (1C, d, J = 3.4), 23.9 (1C, d, J = 3.4), 23.7 (1C, d, J = 5.2), 23.5 (1C, d, J = 5.2), 19.89 (1C, d, J = 1.7); ESI-MS/MS $[M + H^+]$ 422.22.

Synthesis of Nitrone Agm-DIPPMPO 12. *Agm-DIPPMPO 12.* To a mixture of agmantine (0,21 g, 0,84 mmol) in acetonitrile (5 mL) was added NHS-DIPPMPO (0.28 g, 0.64 mmol) in 8 mL of anhydrous acetonitrile followed by the addition of *N*-ethyldiisopropylamine (0.33 mL, 1.94 mmol). The reaction mixture was stirred overnight. The solvent was removed under reduce pressure. Purification of the crude product by flash chromatography on basic alumina (CH_2Cl_2/EtOH 75:25) afforded a pale yellow powder (0.277 g, 95%): ^{31}P NMR (121.49 MHz, D_2O) δ 18.88; ^{1}H NMR (300.13 MHz) δ 7,36 (1H, d, J = 2.8), 4.85−4.75 (2H, m), 4.36−4.29 (1H, m), 4.20−4.14 (1H, m), 3.14−3.05 (4H, m), 2.98−2.60 (3H, m), 1.67 (3H, d, J = 14.9), 1.60−1.50 (4H, m), 1.31−1.26 (12H, m); ^{13}C NMR (75.47 MHz) δ 162.9 ($1C^{IV}$, s), 158.9 (1C, s), 144.3 (1C,d, J = 7.5), 77.3 ($1C^{IV}$, d, J = 153.7), 75.6 (1C, d, J = 7.5), 75.39 (1C, d, J = 8.0), 64.6 (1C, d, J = 2.8), 46.2 (1C, d, J = 2.3), 41.51 (1C, s), 40.6 (1C, s), 30.7 (1C, s), 26.9 (1C, s), 26.0 (1C, s), 24.1 (1C, d, J = 2.9), 24.0 (1C, d, J = 4.0), 23.7 (1C, d, J = 6.9), 23.6 (1C, d, J = 4.6), 19.99 (1C, s); ESI-MS/MS [M + H$^+$] 450.25.

Mitochondrial Uptake Studies. Mitochondria were isolated from rat heart as described by Sethumadhavan et al.[45] Briefly, freshly isolated heart tissue was homogenized in modified Chappell Perry medium: 10 mM HEPES, 100 mM KCl, 1 mM EGTA, 5 mM $MgSO_4$, 1 mM ATP, and 0.2% BSA, pH 7.4. Homogenates were centrifuged at 700*g* for 15 min at 4 °C. The supernatant was transferred to a cold clean tube and subjected to high-speed centrifugation (10 000*g*, 15 min, 4 °C). The final supernatant was discarded, and the mitochondrial pellet was washed twice. Finally, the pellets were resuspended in storage buffer: 10 mM HEPES, 100 mM KCl, and 1 mM EGTA, pH 7.4. Mitochondrial protein was quantified by bicinchoninic acid method and used immediately for uptake assays. Incubations were performed in 10 mM HEPES buffer (pH = 7.2) containing KCl (120 mM), EGTA (1 mM), succinate (5 mM) with 10 μM of the spin trap solution. Aliquots of the supernatant were collected at 0 and 30 min of incubation for HPLC analysis. Aliquots of the initial solutions and samples at time 0 and 30 min were analyzed, and the initial reagent solution after 30 min was also reinjected to confirm the stability of the compounds tested over the course of experiment. After incubation, the mixtures were centrifugated (10 min × 1000*g*, 4 °C), and supernatant was analyzed by HPLC with UV−vis absorption detection.

■ ASSOCIATED CONTENT

Ⓢ Supporting Information

^{1}H, ^{31}P, ^{13}C NMR, and EPR spectra, X-ray data and quantum-mechanical calculations. This material is available free of charge via the Internet at http://pubs.acs.org.

■ AUTHOR INFORMATION

Corresponding Authors

*E-mail: olivier.ouari@univ-amu.fr.

*E-mail: paul.tordo@univ-amu.fr.

Funding

This work was supported by Aix-Marseille University, CNRS, and by "Agence Nationale de la Recherche" (ANR-09-BLAN-0193−02, SPIN BioRad).

Notes

The authors declare no competing financial interest.

■ ACKNOWLEDGMENTS

A.R. thanks the Hungarian Science Fund for partial funding of this work (Grant OTKA T-046953). The authors thank Patrick Bernasconi (Aix-Marseille University) for EPR technical support, and F. Peyrot, J.-L. Boucher, and Y. M. Frapart for discussions.

■ ABBREVIATIONS

DEPMPO, 5-(diethoxyphosphoryl)-5-methylpyrroline *N*-oxide; DIPPMPO, 5-(diisopropyloxyphosphoryl)-5-methylpyrroline *N*-oxide; DMPO, 5,5-dimethylpyrroline *N*-oxide; NHS-DIPPMPO, (*N*-hydroxysuccinimidyl-DIPPMPO); EMPO, 5-ethoxycarbonyl-5-methylpyrroline *N*-oxide; HX, hypoxanthine; Mito-DIPPMPO, (4*R**,5*R**)-5-(diisopropyloxyphosphoryl)-5-methyl-4-[({[2-(triphenylphosphonio)ethyl]carbamoyl}oxy)-methyl]pyrroline *N*-oxide bromide; $Mito_{10}$-DEPMPO, (4*R**,5*R**)-5-(diethoxyphosphoryl)-5-methyl-4-[({[2-(triphenylphosphonio)decyl]carbamoyl}oxy)methyl]pyrroline *N*-oxide bromide; $Mito_5$-DIPPMPO, (4*R**,5*R**)-5-(diisopropyloxyphosphoryl)-5-methyl-4-[({[2-(triphenylphosphonio)pentyl]carbamoyl}oxy)methyl]pyrroline *N*-oxide bromide; Mito-bis-DIPPMPO, (4*R**,5*R**)-5-(diisopropyloxyphosphoryl)-5-methyl-4-[({bis[2-(triphenylphosphonio)ethyl]-carbamoyl}oxy)methyl]pyrroline *N*-oxide bromide; TrA-DEPMPO, 5-(diethoxyphosphoryl)-5-methyl-4-[({trityl-2-azaethyl}carbamoyl)oxymethyl]pyrroline *N*-oxide; Gua-DIPPMPO, 5-(diisopropyloxyphosphoryl)-5-methyl-4-[({[2-(guanidino)ethyl]carbamoyl}oxy)methyl]-5-methyl-1-pyrroline *N*-oxide; Agm-DIPPMPO, 5-(diisopropyloxyphosphoryl)-5-methyl-4-[({[2-(guanidino)buthyl]carbamoyl}oxy)methyl]-5-methyl-1-pyrroline *N*-oxide; SOD, superoxide dismutase; XO, xanthine oxidase; ROS, reactive oxygen; RNS, reactive nitrogen species

■ REFERENCES

(1) Pryor, W. A., Houk, K. N., Foote, C. S., Fukuto, J. M., Ignarro, L. J., Squadrito, G. L., and Davies, K. J. A. (2006) Free radical biology and medicine: it's a gas, man! *Am. J. Physiol. 291*, R491−R511.

(2) Floyd, R. A. (2009) Serendipitous findings while researching oxygen free radicals. *Free Radical Biol. Med. 46*, 1004−1013.

(3) Halliwell, B., and Gutteridge, J. M. C. (2007) *Free Radicals in Biology and Medicine*, 4th ed., Oxford University Press, Cary, NC.

(4) Hadfield, K. A., Pattison, D. I., Brown, B. E., Hou, L. M., Rye, K. A., Davies, M. J., and Hawkins, C. L. (2013) Myeloperoxidase-derived oxidants modify apolipoprotein A-I and generate dysfunctional high-density lipoproteins: comparison of hypothiocyanous acid (HOSCN) with hypochlorous acid (HOCI). *Biochem. J. 449*, 531−542.

(5) Vasquez-Vivar, J. (2009) Tetrahydrobiopterin, superoxide, and vascular dysfunction. *Free Radical Biol. Med. 47*, 1108−1119.

(6) Wright, R. M., McManaman, J. L., and Repine, J. E. (1999) Alcohol-induced breast cancer: a proposed mechanism. *Free Radical Biol. Med. 26*, 348−354.

(7) Lin, M. T., and Beal, M. F. (2006) Mitochondrial dysfunction and oxidative stress in neurodegenerative diseases. *Nature 443*, 787−795.

(8) Schriner, S. E., Linford, N. J., Martin, G. M., Treuting, P., Ogburn, C. E., Emond, M., Coskun, P. E., Ladiges, W., Wolf, N., Van Remmen, H., Wallace, D. C., and Rabinovitch, P. S. (2005) Extension of murine life span by overexpression of catalase targeted to mitochondria. *Science 308*, 1909−1911.

(9) Zielonka, J., Zielonka, M., Sikora, A., Adamus, J., Joseph, J., Hardy, M., Ouari, O., Dranka, B. P., and Kalyanaraman, B. (2012) Global profiling of reactive oxygen and nitrogen species in biological systems. *J. Biol. Chem. 287*, 2984−2995.

(10) Wardman, P. (2007) Fluorescent and luminescent probes for measurement of oxidative and nitrosative species in cells and tissues: progress, pitfalls, and prospects. *Free Radical Biol. Med. 43*, 995−1022.

(11) Vasquez-Vivar, J., Kalyanaraman, B., Martasek, P., Hogg, N., Masters, B. S. S., Karoui, H., Tordo, P., and Pritchard, K. A. (1998) Superoxide generation by endothelial nitric oxide synthase: the influence of cofactors. *Proc. Natl. Acad. Sci. U.S.A. 95*, 9220−9225.

(12) Buettner, G. R., and Mason, R. P. (1990) Spin-trapping methods for detecting superoxide and hydroxyl free-radicals in-vitro and in-vivo. *Methods Enzymol. 186*, 127−133.

(13) Velayutham, M., Hemann, C., and Zweier, J. L. (2011) Removal of H_2O_2 and generation of superoxide radical: role of cytochrome *c* and NADH. *Free Radical Biol. Med. 51*, 160−170.
(14) Mitchell, D. G., Rosen, G. M., Tseitlin, M., Symmes, B., Eaton, S. S., and Eaton, G. R. (2013) Use of rapid-scan EPR to improve detection sensitivity for spin-trapped radicals. *Biophys. J. 105*, 338−342.
(15) Hawkins, C. L., and Davies, M. J. (2013) Detection and characterisation of radicals in biological materials using EPR methodology. *Biochim. Biophys. Acta 840*, 708−721.
(16) Hardy, M., Chalier, F., Ouari, O., Finet, J. P., Rockenbauer, A., Kalyanaraman, B., and Tordo, P. (2007) Mito-DEPMPO synthesized from a novel NH_2-reactive DEPMPO spin trap: a new and improved trap for the detection of superoxide. *Chem. Commun.*, 1083−1085.
(17) Frejaville, C., Karoui, H., Tuccio, B., Lemoigne, F., Culcasi, M., Pietri, S., Lauricella, R., and Tordo, P. (1995) 5-(Diethoxy-phosphoryl)-5-methyl-1-pyrroline *N*-oxide—a new efficient phosphorylated nitrone for the in-vitro and in-vivo spin-trapping of oxygen-centered radicals. *J. Med. Chem. 38*, 258−265.
(18) Olive, G., Mercier, A., Le Moigne, F., Rockenbauer, A., and Tordo, P. (2000) 2-Ethoxycarbonyl-2-methyl-3,4-dihydro-2*H*-pyrrole-1-oxide: evaluation of the spin trapping properties. *Free Radical Biol. Med. 28*, 403−408.
(19) Kim, S. U., Liu, Y., Nash, K. M., Zweier, J. L., Rockenbauer, A., and Villamena, F. A. (2010) Fast reactivity of a cyclic nitrone-calix[4]pyrrole conjugate with superoxide radical anion: theoretical and experimental studies. *J. Am. Chem. Soc. 132*, 17157−17173.
(20) Villamena, F., Gallucci, J., Velayutham, M., Hadad, C., and Zweier, J. (2003) Spin trapping by 5-carbamoyl-5-methyl-1-pyrroline *N*-oxide (AMPO): theoretical and experimental studies. *Free Radical Biol. Med. 35*, S15−S15.
(21) Finkelstein, E., Rosen, G. M., and Rauckman, E. J. (1980) Spin trapping—kinetics of the reaction of superoxide and hydroxyl radicals with nitrones. *J. Am. Chem. Soc. 102*, 4994−4999.
(22) Finkelstein, E., Rosen, G. M., and Rauckman, E. J. (1982) Production of hydroxyl radical by decomposition of superoxide spin-trapped adducts. *Mol. Pharmacol. 21*, 262−265.
(23) Hardy, M., Bardelang, D., Karoui, H., Rockenbauer, A., Finet, J. P., Jicsinszky, L., Rosas, R., Ouari, O., and Tordo, P. (2009) Improving the trapping of superoxide radical with a *β*-cyclodextrin-5-diethoxy-phosphoryl-5-methyl-1-pyrroline-*N*-oxide (DEPMPO) conjugate. *Chem.—Eur. J. 15*, 11114−11118.
(24) Smith, R. A. J., Hartley, R. C., and Murphy, M. P. (2011) Mitochondria-targeted small molecule therapeutics and probes. *Antioxid. Redox Signaling 15*, 3021−3038.
(25) Hoye, A. T., Davoren, J. E., Wipf, P., Fink, M. P., and Kagan, V. E. (2008) Targeting mitochondria. *Acc. Chem. Res. 41*, 87−97.
(26) Sheu, S. S., Nauduri, D., and Anders, M. W. (2006) Targeting antioxidants to mitochondria: a new therapeutic direction. *Biochim. Biophys. Acta, Mol. Basis Dis. 1762*, 256−265.
(27) Szewczyk, A., and Wojtczak, L. (2002) Mitochondria as a pharmacological target. *Pharmacol. Rev. 54*, 101−127.
(28) Smith, R. A. J., Porteous, C. M., Coulter, C. V., and Murphy, M. P. (1999) Selective targeting of an antioxidant to mitochondria. *Eur. J. Biochem. 263*, 709−716.
(29) Robertson, L., and Hartley, R. C. (2009) Synthesis of *N*-arylpyridinium salts bearing a nitrone spin trap as potential mitochondria-targeted antioxidants. *Tetrahedron 65*, 5284−5292.
(30) James, A. M., Cocheme, H. M., Smith, R. A. J., and Murphy, M. P. (2005) Interactions of mitochondria-targeted and untargeted ubiquinones with the mitochondrial respiratory chain and reactive oxygen species: implications for the use of exogenous ubiquinones as therapies and experimental tools. *J. Biol. Chem. 280*, 21295−21312.
(31) Adlam, V. J., Harrison, J. C., Porteous, C. M., James, A. M., Smith, R. A. J., Murphy, M. P., and Sammut, I. A. (2005) Targeting an antioxidant to mitochondria decreases cardiac ischemia-reperfusion injury. *Faseb J. 19*, 1088−1095.
(32) Xu, Y. K., and Kalyanaraman, B. (2007) Synthesis and ESR studies of a novel cyclic nitrone spin trap attached to a phosphonium group: a suitable trap for mitochondria-generated ROS? *Free Radical Res. 41*, 1−7.
(33) Quin, C., Trnka, J., Hay, A., Murphy, M. P., and Hartley, R. C. (2009) Synthesis of a mitochondria-targeted spin trap using a novel Parham-type cyclization. *Tetrahedron 65*, 8154−8160.
(34) Hardy, M., Rockenbauer, A., Vasquez-Vivar, J., Felix, C., Lopez, M., Srinivasan, S., Avadhani, N., Tordo, P., and Kalyanaraman, B. (2007) Detection, characterization, and decay kinetics of ROS and thiyl adducts of Mito-DEPMPO spin trap. *Chem. Res. Toxicol. 20*, 1053−1060.
(35) Rockenbauer, A., and Korecz, L. (1996) Automatic computer simulations of ESR spectra. *Appl. Magn. Reson. 10*, 29−43.
(36) Clement, J. L., Ferre, N., Siri, D., Karoui, H., Rockenbauer, A., and Tordo, P. (2005) Assignment of the EPR spectrum of 5,5-dimethyl-1-pyrroline *N*-oxide (DMPO) superoxide spin adduct. *J. Org. Chem. 70*, 1198−1203.
(37) Rockenbauer, A., Clement, J. L., Culcasi, M., Mercier, A., Tordo, P., and Pietri, S. (2007) Combined ESR and thermodynamic studies of the superoxide adduct of 5-(diethoxyphosphoryl)-5-methyl-1-oyrroline *N*-oxide (DEPMPO): hindered rotation around the O−O bond evidenced by two-dimensional simulation of temperature-dependent spectra. *J. Phys. Chem. A 111*, 4950−4957.
(38) Houriez, C., Ferre, N., Siri, D., Tordo, P., and Masella, M. (2010) Structure and spectromagnetic properties of the superoxide radical adduct of DMPO in water: elucidation by theoretical investigations. *J. Phys. Chem. B 114*, 11793−11803.
(39) Hausladen, A., and Fridovich, I. (1993) Competitive-inhibition of xanthine-oxidase by guanidinium: dependence upon monovalent anions and effects on production of superoxide. *Arch. Biochem. Biophys. 304*, 479−482.
(40) Ross, M. F., Da Ros, T., Blaikie, F. H., Prime, T. A., Porteous, C. M., Severina, I. I., Skulachev, V. P., Kjaergaard, H. G., Smith, R. A. J., and Murphy, M. P. (2006) Accumulation of lipophilic dications by mitochondria and cells. *Biochem. J. 400*, 199−208.
(41) Hardy, M., Chalier, F., Ouari, O., Finet, J. P., Rockenbauer, A., Kalyanaraman, B., and Tordo, P. (2007) Mito-DEPMPO synthesized from a novel NH_2-reactive DEPMPO spin trap: a new and improved trap for the detection of superoxide. *Chem. Commun.*, 1083−1085.
(42) Zon, J. (1984) Synthesis of diisopropyl 1-nitroalkane-phosphonates from diisopropyl 1-oxoalkanephosphonate. *Synthesis 8*, 661−663.
(43) Li, S., Zhou, X., Wang, L., Xu, C., Ruan, C., Lin, C., Xiao, J., Zheng, Z., Liu, H., Xie, Y., Zhong, W., and Cui, H. (2005) Preparation of tyrosine derivs. substituted by alkanoyl as hPPAR*α* and & hPPAR*γ* agonists. PCT Int. Appl. WO2005116018 (A1).
(44) McAllister, P. R., Dotson, M. J., Grim, S. O., and Hillman, G. R. (1980) Effects of phosphonium compounds on schistosoma mansoni. *J. Med. Chem. 23*, 862−865.
(45) Sethumadhavan, S., Vasquez-Vivar, J., Migrino, R. Q., Harmann, L., Jacob, H. J., and Lazar, J. (2012) Mitochondrial DNA variant for complex I reveals a role in diabetic cardiac remodeling. *J. Biol. Chem. 287*, 22174−22182.

■ NOTE ADDED AFTER ASAP PUBLICATION

This article was published ASAP on June 13, 2014. Author affiliations have been updated and the corrected version was reposted on June 23, 2014.